ELSEVIER

International Journal of Minerals, Metallurgy and Materials
Volume 16, Number 1, February 2009, Page 19

Minerals

Fractal analysis on the spatial distribution of acoustic emission in the failure process of rock specimens

Rui-fu Yuan[1)] *and Yuan-hui Li*[2)]

1) Energy Science and Engineering School, Henan Polytechnic University, Jiaozuo 454000, China
2) College of Resource and Civil Engineering, Northeastern University, Shenyang 110004, China
(Received 2008-02-02)

Abstract: The spatial distribution of acoustic emission (AE) events in the failure process of several rock specimens was acquired using an advanced AE acquiring and analyzing system. The box counting method (BCM) was employed to calculate the fractal dimension (FD) of AE spatial distribution. There is a similar correlation between the fractal dimension and the load strength for different rock specimens. The fractal dimension presents a decreasing trend with the increase of load strength. For the same kind of specimens, their FD values will decrease to the level below a relatively same value when they reach failure. This value can be regarded as the critical value, which implies that the specimen will reach failure soon. The results reflect that it is possible to correlate the damage of rock with a macroscopic parameter, the FD value of AE signals. Furthermore, the FD value can be also used to forecast the final failure of rock. This conclusion allows identifying or predicting the damage in rock with a great advantage over the classic theory and is very crucial for forecasting rockburst or other dynamic disasters in mines.

Key words: rockburst; acoustic emission; spatial distribution; fractal dimension; critical value; damage

[*This work was financially supported by the Special Subject of the National High-Tech Research and Development Program of China (No.2007AA06Z107), Supporting Project of New Century Excellence Talents in Chinese Universities (No.NCET-07-0163), Opening Research Foundation of CAS Key Laboratory of Rock and Soil Mechanics (No.Z110607) and Youth Foundation of Henan Polytechnic University (No.Q2008-51).*]

1. Introduction

Rock is a typically inhomogenous and anisotropic material, which contains several natural defects with various scales, such as microcracks, pores, fissures, joints inclusions, and precipitates. Large numbers of acoustic emission (AE) signals will be generated when rock is loaded till failure. Since AE signals are generated by propagating and expanding of microcracks, each AE signal contains plentiful information of structure change inside the rock [1-3]. Therefore, it is not surprising that in geological science, the acoustic emission phenomenon has attracted considerable attention of rock engineering researchers [4-7]. Owing to facility and technical reasons, early AE studies in rock engineering were limited to the statistics of AE number, counts, energy, and magnitude [8-9]. The spatial distribution of AE events reflects the propagation of microcracks inside the rock, and therefore, it is worth more than the simple statistic parameters. With the rapid development of location technique, the research on the spatial distribution of AE sources emerged after the 1990s. Fox example, Lockner [10] observed the complete nucleation and growth process of a fault from the locations of AE events. Xu *et al*. [11] preliminarily analyzed the temporal and spatial distribution of microcracks in several specimens using an 8-channel, high-speed AE signal sampling and analyzing system. Li *et al*. [12] achieved the 3-dimensional distribution of AE events during the whole failure process of rock specimens under uniaxial compression and observed the emergence and filling process of the gap.

However, since the AE distribution is extremely disorderly, it is difficult to establish the bridge between the distribution of AE events and the macro-mechanical behavior of rock. In recent years,

Corresponding author: Rui-fu Yuan, **E-mail:** yrf@hpu.edu.cn
Also available online at www.sciencedirect.com

fractal geometry has been widely used to describe some irregular phenomena in the fracture behavior of materials. Biancolini *et al*. [13] used fractal analysis and the box-counting method to characterize the spatial distribution of the prime AE sources through the fractal dimension. Nanjo [14] researched the relationship between the fractal dimensions of spatial distribution of aftershocks and the pre-existing active faults. Xie [15] founded the fractal rock mechanics and analyzed the fractal dimension of spatial distribution of microseism events before a main rockburst in Galena Mine, USA. However, till now, only a few successful cases forecasting rockburst by microseism technique indicate that the understanding and knowledge of the mechanical behavior of AE distribution in rock still remains in the primary stage and cannot yet fully meet the needs of engineering design. As a result, the further investigation of the laws of damage evolution and the mechanisms of AE distribution has theoretical and practical significance.

The aim of this article was to propose a new diagnostic methodology based on data processing of AE signals for the study of microcrack nucleation and propagation in rock. The result of fractal analysis by the box-counting method (BCM) in particular is the characterization of the signal from the point of view of the spatial distribution of the prime AE sources. From BCM, it was possible to extract a parameter (fractal dimension) that could be correlated with the damage of the material.

2. Experimental procedure

2.1. Specimens

Several kinds of brittle rock, such as granite, marble, and limestone were chosen and processed to specimens to meet the requirements suggested by ISRM. Table 1 shows the specification of the specimens used in the test.

Table 1. Specification of the specimens

Serial number	Lithology	Size	Wave velocity / ($m \cdot s^{-1}$)	Home
UG-1	Granite	92 mm×101 mm×151 mm	4100	Yiwulü Mountain
UG-2	Granite	99 mm×100 mm×151 mm	4500	Yiwulü Mountain
UG-3	Granite	100 mm×103 mm×151 mm	3800	Yiwulü Mountain
UG-4	Granite	102 mm×103 mm×151 mm	4400	Yiwulü Mountain
UG-5	Granite	92 mm×102 mm×150 mm	3500	Yiwulü Mountain
UG-8	Granite	71 mm×75 mm×154 mm	4500	Yiwulü Mountain
US-1	Sandstone	ϕ 80 mm×182 mm	5100	Zhaogu Coal Mine
US-2	Sandstone	ϕ 65 mm×101 mm	4300	Zhaogu Coal Mine
US-3	Sandstone	ϕ 64 mm×102 mm	3000	Zhaogu Coal Mine
US-4	Sandstone	ϕ 66 mm×102 mm	3500	Zhaogu Coal Mine
UM-1	Marble	61 mm×61 mm×151 mm	6000	Nanyang
UM-2	Marble	62 mm×63 mm×128 mm	6100	Nanyang
UM-3	Marble	ϕ 60 mm×118 mm	4200	Nanyang
UM-4	Marble	ϕ 61 mm×120 mm	4000	Nanyang
UD-1	Dolerite	ϕ 56 mm×125 mm	5100	Hongtoushan Copper Mine
UD-2	Dolerite	ϕ 56 mm×126 mm	5000	Hongtoushan Copper Mine
UD-3	Dolerite	ϕ 56 mm×125 mm	5000	Hongtoushan Copper Mine
UD-4	Dolerite	ϕ 56 mm×124 mm	4100	Hongtoushan Copper Mine
UD-5	Dolerite	ϕ 56 mm×124 mm	4100	Hongtoushan Copper Mine

2.2. Acoustic emission monitoring

Monitoring of AE signals was achieved using eight piezoelectric sensors with response frequencies at 125 to 750 kHz. These sensors were positioned on the sides of specimens and were coupled with silicone grease. The signals were amplified with pre-amplifiers (40 dB) and main amplifiers (0-20 dB, auto-adjustive). A PC with AE analyzing software was used for the acquisition and memorization of AE signals. Fig. 1 shows the arrangement of the experimental equipments.

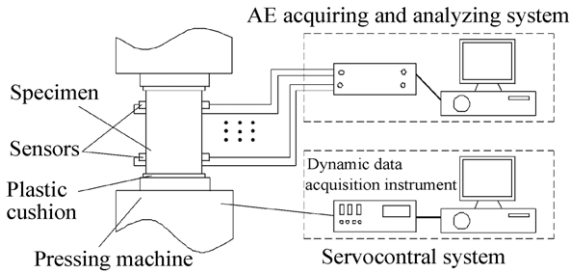

Fig. 1. Arrangement of the experimental instruments.

2.3. Experimental results

Fig. 2 plots the AE rate and the load versus displacement of UG-1 specimen. It reports signals with frequencies between 125 and 750 kHz. It can be seen from Fig. 2 that as the load increases, the intensity of AE signals grows accordingly. The greatest emission, expressed by AE rate and energy intensity, occurs when the load approaches the maximum level of 400 kN. Fig. 3 shows the spatial distribution of AE signals during the load process for UG-1 specimen. It can be observed in Figs. 2 and 3 that the AE events show the following stages, which are similar to those in Figs. 4-6. In the first stage (<20% of peak load), the rate of AE events presents a low value and most of these events are located at the two ends of the specimens. In the second stage (20%-80% of the peak load), the AE rate increases stably, and the location of AE events gradually extends to the center area of the specimen from the two ends. A gap with few AE events is formed in the center area of the specimen. In the third stage (>80% of peak load), the intensity of AE signals rises drastically till the specimen failure, and most of these AE events appear in the specimen's center area and fill the gap.

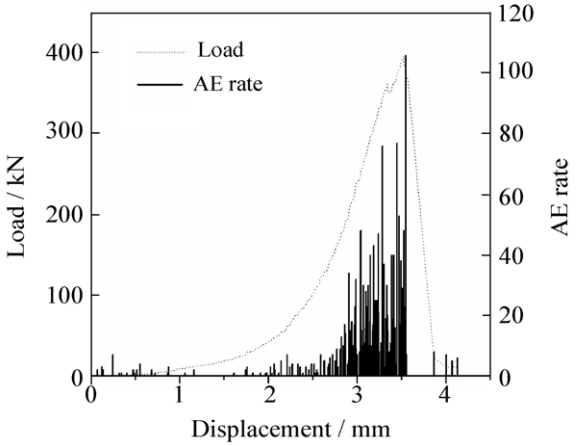

Fig. 2. Load and AE rate *vs.* displacement for the UG-1 specimen.

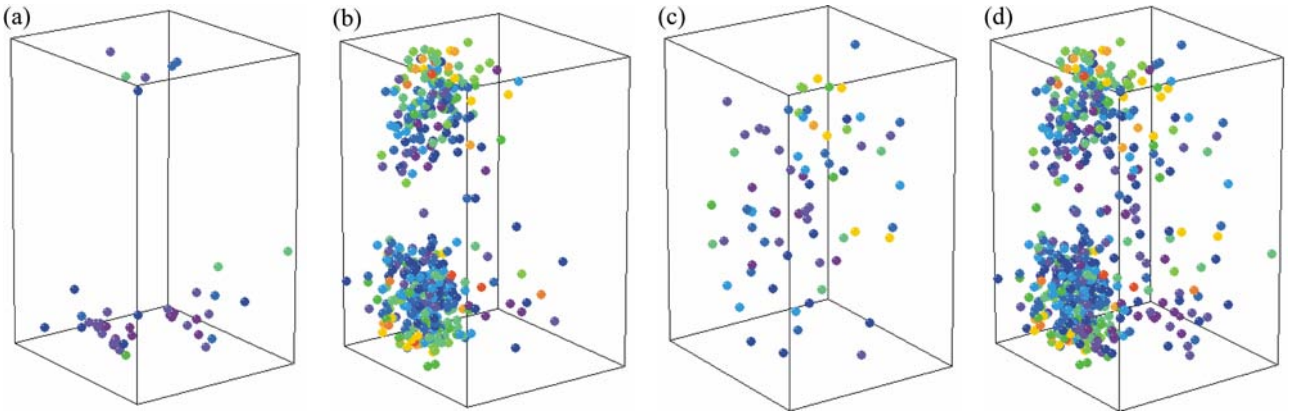

Fig. 3. Spatial distribution of AE signals in different stages of load process for the UG-1 specimen: (a) 0-20% of peak load; (b) 20%-80% of peak load; (c) 80%-100% of peak load; (d) whole process.

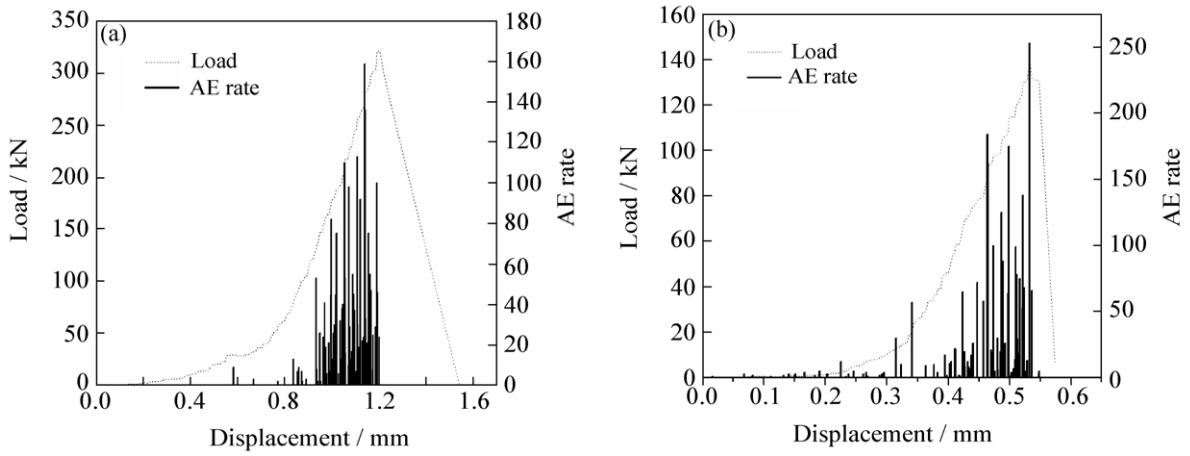

Fig. 4. Load and AE rate *vs.* displacement for different specimens: (a) US-1; (b) UM-1.

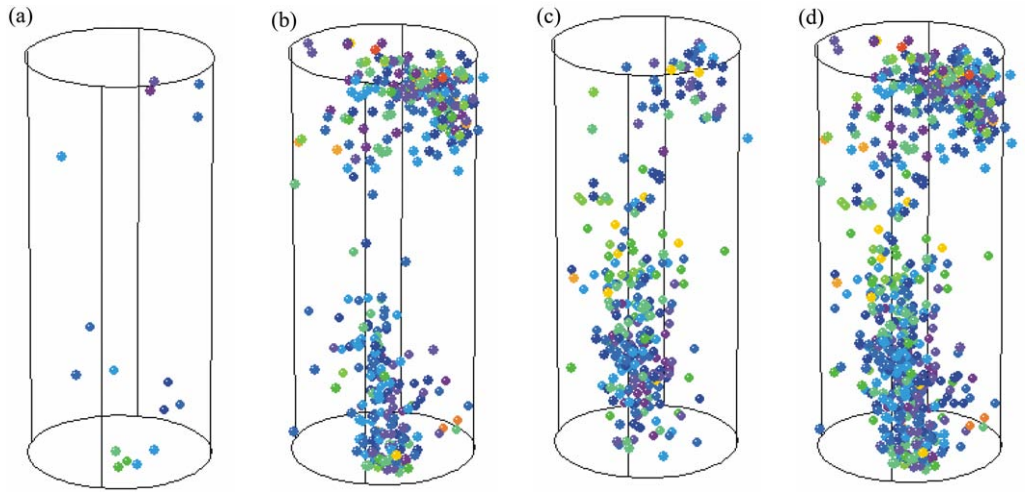

Fig. 5. Spatial distribution of AE signals in different stages of load process for US-1 specimen: (a) 0-20% of peak load; (b) 20%-80% of peak load; (c) 80%-100% of peak load; (d) whole process.

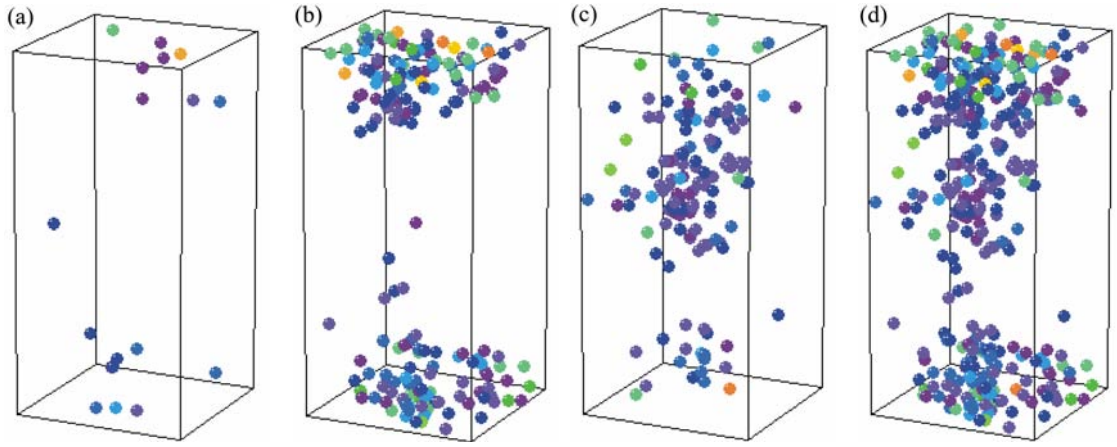

Fig. 6. Spatial distribution of AE signals in different stages of load process for UM-1 specimen: (a) 0-20% of peak load; (b) 20%-80% of peak load; (c) 80%-100% of peak load; (d) whole process.

3. Fractal dimension of spatial distribution of AE events

Data processing of AE signals was achieved through the fractal algorithm using, in particular, the box-counting method, described below.

The space that the specimen occupies could be covered by cubes with the side length of r. Then, some cubes were empty and some others contain AE events. It indicated that these unempty cubes covered the spatial distribution of AE signals. The unempty cubes were counted and recorded as $N(r)$. When $r \to 0$, the fractal dimension could be calculated as follows:

$$D_{\mathrm{B}} = \lim_{r \to 0} \frac{\lg N(r)}{-\lg r}.$$

However, the set of AE events was composed of limited points. When r was lower than the value $|U|$ ($|U|=\inf\{|X-Y|: X, Y \in U\}$, where U is the set of AE events), $N(r)$ will be a constant value, which is the total number of AE events. Therefore, in practical operation, the usual method was to find a series values of r and $N(r)$ and drew the $\lg N(r)$ to $\lg 1/r$ line in lg-lg grid. The slope of the $\lg N(r)$ to $\lg 1/r$ line was the fractal dimension value D_{B}.

4. Results and discussion

As mentioned above, the activity of AE events, especially AE spatial distribution, reflected the evolvement of damage inside the specimen. Several researches indicated that the behaviors of rock material, such as the distribution of microcracks, the shape of fracture surface, and the envelopment of damage, showed the fractal character. Of course, the disorderly distribution of AE signals generated in the failure process also had the fractal character.

Figs. 7-10 show the correlation between the fractal dimension and the load strength of the specimens of granite, sandstone, marble, and dolerite, respectively. There is a similar correlation between the fractal dimension and the load strength for all tests. The fractal dimension shows a decreasing trend with the increase of load strength. The whole load process is divided into 5 stages. In the first stage of the load process

(<20% of peak load), the fractal dimension remains high in a range of 0.45-0.85. This implies that during the initial damage of the specimens, there is no organization in the spatial distribution of AE events, and therefore, there is no organization or nucleation of microcracks inside the specimens. Moreover, after the first half of the load process, the fractal dimension begins to decrease, reaching D_B <0.3 or 0.4 at the failure point. It is possible to correlate the fatigue damage with the distribution of AE events, showing that the nucleation and propagation of cracks begin after the first half of the total load process. The most exciting phenomenon is that the FD values will descend to the level below a critical value for the same kind of specimens when they approach failure (at >80% of peak load), such as 0.3 for granite and sandstone specimens and 0.4 for dolerite and marble specimens (notice the dashed line in Figs. 7-10). The FD values of the specimens in different load stages are reported in Table 2.

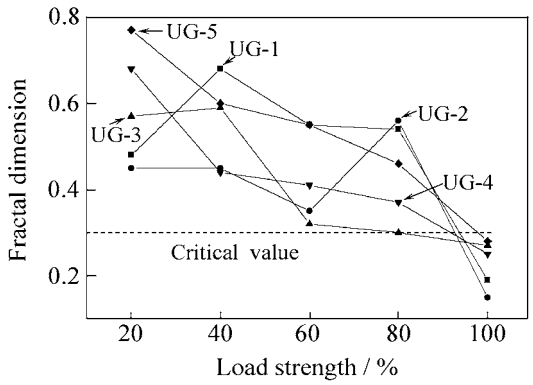

Fig. 7. Values of fractal dimension in failure process for 5 granite specimens.

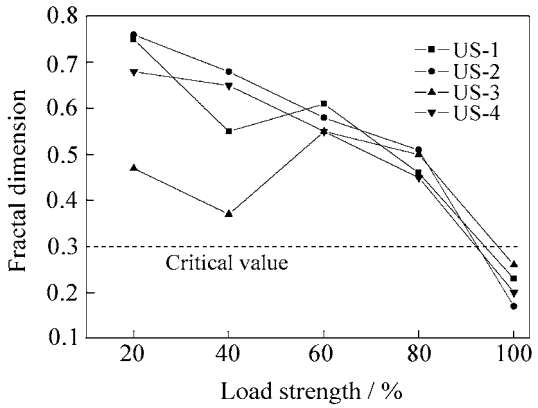

Fig. 8. Values of fractal dimension in failure process for 4 sandstone specimens.

The decrease of fractal dimension implies that the sources of emission are ordering. They will assemble on a plane (or several planes sometimes). The plane(s) is just the position of macro-cracks which lead to the completely failure of the specimen. It is possible to notice that all specimens' FD values decrease to the level below a relatively same value when the specimens reach failure. This value can be regarded as the critical value, which implies that the specimen will reach failure soon.

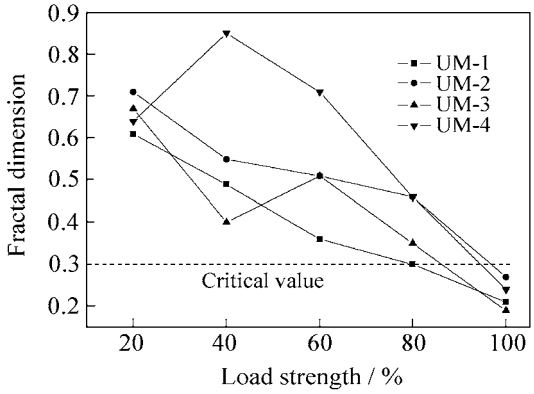

Fig. 9. Values of fractal dimension in failure process for 4 marble specimens.

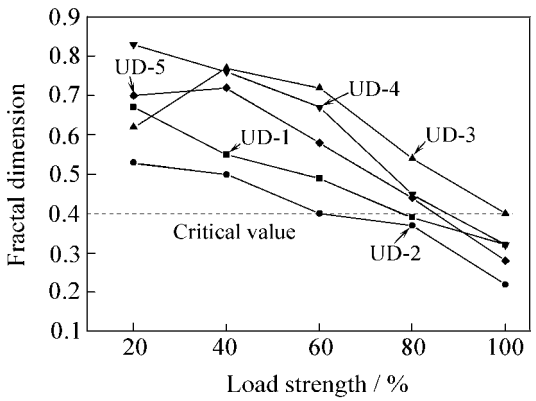

Fig. 10. Values of fractal dimension in failure process for 5 dolerite specimens.

5. Conclusion

It is seen in this article that it is possible to correlate the damage of the material with a macroscopic parameter, namely the fractal dimension of AE signals. This result suggests that it is possible to use the fractal analysis of AE signals as a valuable diagnostic methodology for the study of microcrack nucleation and propagation in rock. The tests emphasize a relationship between the damage during a load process and the fractal dimension of AE signals. Furthermore, the results can be repeated by changing the condition of the test. It is verified that the values of fractal dimension will decrease to a critical value for all tests performed in the final stage. This method allows identifying or predicting the microcracks with a great advantage over the classic theory and is very crucial for forecasting rockburst or other dynamic disasters in mines.

Table 2. Fractal dimension of AE events in different specimens during the uniaxial compressive load process

No.	Load strength					Critical value
	0-20%	20%-40%	40%-60%	60%-80%	80%-100%	
UG-1	0.48	0.68	0.55	0.54	0.19	0.3
UG-2	0.45	0.45	0.35	0.56	0.15	
UG-3	0.57	0.59	0.32	0.31	0.27	
UG-4	0.68	0.44	0.41	0.37	0.25	
UG-5	0.77	0.60	0.55	0.46	0.28	
US-1	0.75	0.55	0.61	0.46	0.23	0.3
US-2	0.76	0.68	0.58	0.51	0.17	
US-3	0.47	0.37	0.55	0.50	0.26	
US-4	0.68	0.65	0.55	0.45	0.20	
UM-1	0.61	0.49	0.36	0.30	0.21	0.3
UM-2	0.72	0.56	0.51	0.46	0.27	
UM-3	0.67	0.40	0.51	0.35	0.19	
UM-4	0.64	0.85	0.71	0.46	0.24	
UD-1	0.67	0.55	0.49	0.39	0.32	0.4
UD-2	0.53	0.5	0.4	0.37	0.22	
UD-3	0.62	0.77	0.72	0.54	0.4	
UD-4	0.83	0.76	0.67	0.45	0.32	
UD-5	0.7	0.72	0.58	0.44	0.28	

Acknowledgements

The authors would like to thank Mr. J. Tian, J.P. Liu, and J.Y. Zhang for their help in the tests, and Prof. Y.J. Wang for correcting the language.

References

[1] D.J. Holcomb, Summary of discussions on behaviour of solids with a system of cracks, [in] *Mechanies of Geomaterials: Rocks, Concretes, Soils*, New York, 1985, p.71.

[2] K. Kurita and N. Fujii, Stress memory of crystalline rocks in acoustic emission, *Geophys. Res. Lett.*, 6(1979), No.1, p.9.

[3] M. Chen, Z.X. Chen, and Y. Jin, Determination of *in-situ* stresses at great depth by using acoustic emission technique of inclined core, *Chin. J. Rock Mech. Eng.* (in Chinese), 17(1998), No.3, p.311.

[4] R.F. Yuan and Y.H. Li, Theoretical and experimental analysis on the mechanism of the Kaiser effect of acoustic emission in brittle rocks, *J. Univ. Sci. Technol. Beijing*, 15(2008), p.1.

[5] F. Han, H.G. Ji, and W. Zhang, Relationship between the acoustic characteristics and damage variable in the process of uniaxial loading and unloading, *J. Univ. Sci. Technol. Beijing* (in Chinese), 29(2007), p.452.

[6] F.H. Ren, X.P Lai, and M.F. Cai, Dynamic destabilization analysis based on AE experiment of deep-seated, steep-inclined and extra-thick coal seam, *J. Univ. Sci. Technol. Beijing*, 15(2008), p.215.

[7] M. Cai, H. Morioka, and P.K. Kaiser, Back-analysis of rock mass strength parameters using AE monitoring data, *Int J. Rock Mech. Min. Sci*, 44(2007), p.538.

[8] R.E. Goodman, Sub audible noise during compression of rock, *Geo. Soc. Am. Bull.*, 74(1963), p.487.

[9] C. Li and E. Norlund, Experimental verification of the Kaiser effect in rock, *Rock Mech. Rock Eng.*, 26(1993), No.4, p.333.

[10] D. Lockner, The role of acoustic emission in the study of rock fracture, *Int. J. Rock Mech. Min. Sci. Geomech. Abstr.*, 30(1993), No.7, p.883.

[11] Z.Y. Xu, S.R. Mei, C.T. Zhuang, *et al*., Preliminary location of microcracks in several rock specimens under true triaxial compression, *Acta Seismol. Sin.*, 7(1994), Suppl., p.51.

[12] Y.H. Li, R.F. Yuan, and X.D. Zhao, Failure process of rock sample observed by AE source locating technique under uniaxial compression, *Key Eng. Mater.*, 324-325(2006), p.567.

[13] M.E. Biancolini, C. Brutti, G. Paparo, and A. Zanini, Fatigue cracks nucleation on steel, acoustic emission and fractal analysis, *Int. J. Fatigue*, 28(2006), p.1820.

[14] K. Nanjo and H. Nagahama, Fractal properties of spatial distributions of aftershocks and active faults, *Chaos Solitons Fractals*, 19(2004), p.387.

[15] H.P. Xie, *Fractals in Rock Mechanics*, A. A. Balkema Publishers, Rotterdam, 1993.